第 35 卷第 1 期
2019 年 1 月

无 机 化 学 学 报
CHINESE JOURNAL OF INORGANIC CHEMISTRY

Vol.35 No.1
165-173

两个基于 Cd(Ⅱ)金属有机骨架化合物在金属离子和有机分子发光传感中的应用

张春丽
(宿州学院化学化工学院,宿州 234000)

摘要:合成了 2 个镉(Ⅱ)金属有机骨架化合物{[Cd(L)(fma)]·0.5H_2O}$_n$ (**1**)和{[Cd(L)$_{0.5}$(sdb)]·DMF}$_n$ (**2**)(L=*E*,*E*-2,5-二己氧基-1,4-双(2-乙烯-吡啶基)苯,H_2fma=延胡酸,H_2sdb=4,4′-磺酰基二苯甲酸),研究了它们在金属离子和有机分子的发光传感中的应用。结果表明,Fe^{3+}对配位聚合物 **1** 和 **2** 的发光强度有明显的猝灭作用。此外,聚合物 **1** 和 **2** 还对水杨醛具有明显的猝灭能力。

关键词:金属有机骨架;发光传感;合成
中图分类号:O614.24$^+$2 **文献标识码**:A **文章编号**:1001-4861(2019)01-0165-09
DOI:10.11862/CJIC.2019.021

Two Cd(Ⅱ)-Based Metal-Organic Frameworks for Luminescence Sensing of Metal Ions and Organic Molecules

ZHANG Chun-Li
(*School of Chemistry and Chemical Engineering, Suzhou University, Suzhou, Anhui* 234000, *China*)

Abstract: Two cadmium metal-organic frameworks, {[Cd(L)(fma)]·0.5H_2O}$_n$ (**1**) and {[Cd(L)$_{0.5}$(sdb)]·DMF}$_n$ (**2**) (L=*E*,*E*-2,5-dihexyloxy-1,4-bis-(2-pyridin-vinyl)benzene, H_2fma =fumaric acid, H_2sdb =4,4′ -sulfonyldibenzoic acid), have been hydrothermally synthesized. Their applications in luminescence sensing of metal anions and organic molecules were explored. The results show that Fe^{3+} has a significant quenching influence on the luminescence intensity of MOFs **1** and **2**. In addition, MOFs **1** and **2** also show some luminescence quenching ability on salicylaldehyde. CCDC: 1828500, **1**; 1544271, **2**.

Keywords: metal-organic framework; luminescence sensing; synthesis

In recent years, metal-organic frameworks (MOFs) have attracted quite a few attentions because of their fascinating structures and properties. They have applications in a wide range of fields, such as gas storage and separation[1-3], luminescence[4-6] and catalysis[7-10]. As we all know, Fe^{3+} is abundant in the industrial water. Though Fe^{3+} is low toxicity for people and animals, high Fe^{3+} concentration will change the sensory properties of water and lead to environmental contamination. Salicylaldehyde is used widely both in organic and drug synthesis as an important intermediate product. However, it is irritating to the respiratory tract or eyes, and induces cough or chest pain after inhalation. Thus, detecting them in the environment effectively has drawn much attention. Recent studies show that the fluorescence method based on the luminescent metal-organic frameworks (MOFs) has special advantages, such as high sensitivity, quick

收稿日期:2018-09-17。收修改稿日期:2018-11-06。
国家自然科学基金(No.21771101)、安徽省大学生创新创业训练计划入选项目(No.201710379129)和宿州学院产学研项目(No.2015hx016)资助。
E-mail:zhangsz1966@163.com

response time, and actual time monitoring[11-15].

In this work, we report two new cadmium metal-organic frameworks (MOFs), $\{[Cd(L)(fma)]\cdot 0.5H_2O\}_n$ (**1**), $\{[Cd(L)_{0.5}(sdb)]\cdot DMF\}_n$ (**2**), (L=*E*,*E*-2,5-dihexyloxy-1,4-bis-(2-pyridin-vinyl)benzene, H_2fma=fumaric acid, H_2sdb=4,4′-sulfonyldibenzoic acid). MOF **1** is a non-interpenetrated 2D+2D → 2D parallel stacked 4-connected sql network with the point symbol of $\{4^4.6^2\}$, while MOF **2** exhibits a interpenetrated 2D+2D → 3D inclined polycatenated 4-connected *sql* network with the point symbol of $\{4^4.6^2\}$. Fluorescence titrations were carried out, and the results confirm that Fe^{3+} ion and salicylaldehyde showed quenching effects on the luminescence of MOFs **1** and **2**. Quenching mechanisms also have been studied.

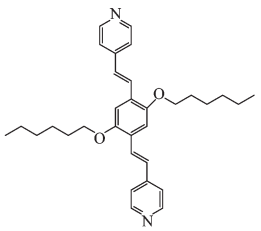

Scheme 1 Structure of ligand L

1 Experimental

1.1 Materials and general methods

The reagents except ligand L were commercial available and were used directly without purification. IR spectra were recorded on a Nicolet (Impact 410) spectrometer with KBr pellets (5 mg of the sample in 300 mg of KBr) in the range of 400~4 000 cm^{-1}. C, H and N elemental analysis was performed with a Perkin Elmer 240C elemental analyzer. The as-synthesized MOF was characterized by thermogravimetric analyses (TGA) on a Perkin Elmer thermogravimetric analyzer, Pyris 1 TGA, from r.t. to 650 K using a heating rate of 10 $K\cdot min^{-1}$ under a N_2 atmosphere. Powder X-ray diffraction (PXRD) measurements were performed on a Bruker D8 Advance X-ray diffractometer by using Cu $K\alpha$ radiation (λ=0.154 18 nm) in the 2θ range of 5°~50°, and the X-ray tube was operated at 40 kV and 40 mA. Fluorescence spectra for the MOFs were conducted with an F-4600 FL Spectrophometer at room temperature.

1.2 Synthesis of L

L was synthesized by the similar procedure previously reported[16]. 1,4-di-bromo-2,5-dihexyloxy-benzene (2.18 g, 5 mmol), 4-vinylpyridine (1.6 g, 15 mmol), $Pd(OAc)_2$ (36 mg, 3% mmol), tris(2,4,6-trimethoxyphenyl) phosphane (106 mg, 4 mmol), Et_3N (5 mL) and CH_3CN (35 mL) were mixed in a 100 mL Schlenk flask and refilled with N_2 three times. The reaction solution was heated at 93 ℃ for three days. The resulting mixture was concentrated *in vacuo*. The crude product was purified with column chromatography on silica gel eluted with petroleum ether/ethyl acetate (1:3, *V*/*V*) to give the product as a yellow solid (2.0 g, 82%). ^1H NMR (400 MHz, $CDCl_3$): δ 8.58 (d, *J*=6.1 Hz, 4H), 7.67 (d, *J*=16.5 Hz, 2H), 7.38 (d, *J*=6.1 Hz, 4H), 7.13 (s, 2H), 7.08 (d, *J*=16.5 Hz, 2H), 4.08 (t, *J*=6.5 Hz, 4H), 1.94~1.84 (m, 4H), 1.61~1.50 (m, 4H), 1.45~1.33 (m, 8H), 0.91 (t, *J*=7.1 Hz, 6H). Anal. Calcd. for L(%): C, 79.30; H, 8.32; N, 5.78. Found (%): C, 79.37; H, 8.29; N, 5.75.

1.3 Syntheses of MOFs

Synthesis of $\{[Cd(L)(fma)]\cdot 0.5H_2O\}_n$ (**1**): A mixture of L (4.8 mg, 0.01 mmol), H_2fma (2.3 mg, 0.02 mmol), $Cd(NO_3)_2\cdot 6H_2O$ (15 mg, 0.1 mmol), DMF (3.0 mL) and H_2O (2.5 mL) was placed in a 20 mL glass vial and heated at 100 ℃ for three days. The resultant orange columnar crystals were washed with fresh DMF, and collected. The yield of the reaction was *ca.* 41% based on L ligand. Elemental analysis calculated for $C_{36}H_{43}CdN_2O_{6.5}$(%): C, 60.04; H, 6.02; N, 3.89. Found (%): C, 60.09; H, 6.09; N, 3.91.

Synthesis of $\{[Cd(L)_{0.5}(sdb)]\cdot DMF\}_n$ (**2**): A mixture of L (4.8 mg, 0.01 mmol), H_2sdb (6.1 mg, 0.02 mmol), $Cd(NO_3)_2\cdot 6H_2O$ (31 mg, 0.1 mmol), DMF (5.0 mL) and H_2O (0.5 mL) was placed in a 20 mL glass vial and heated at 100 ℃ for three days. The resultant orange block crystals were washed with fresh DMF, and collected. The yield of the reaction was *ca.* 46% based on L ligand. Elemental analysis calculated for $C_{33}H_{35}CdN_2O_8S$(%): C, 54.14; H, 4.82; N, 3.83. Found (%): C, 54.25; H, 4.80; N, 3.84.

1.4 X-ray crystallography

Single crystals of MOF **1** and **2** was collected on

a Bruker SMART APEX CCD diffractometer using graphite monochromated Mo $K\alpha$ radiation (λ=0.071 073 nm) at 296 K. Structure solutions were solved by direct methods and the non-hydrogen atoms were located from the trial structures and then refined anisotropically with SHELXTL using full-matrix least-squares procedures based on F^2 values[17]. The hydrogen atom positions were fixed geometrically at calculated distances and allowed to ride on the parent atoms. During the refinement of MOF **1**, the 4-vinylpyridine and hexyloxy groups (C18-C24, N2/C18′-C24′, N2′ and C32-C36/C32′-C36′ atoms) were found to be disordered between two positions, the resulting SOFs (site of occupancies) of these groups were refined to be 0.65/0.35 and 0.5/0.5, respectively. And some needed restraints (DFIX, SADI and SIMU) were applied to ensure a reasonable refinement of this disorder model. Two level A alerts were reported in CheckCIF report, both of which majorly reflect the disorder nature of this structure. The corresponding responses have been embedded into the final CIF file. The crystal and refined data are collected in Table 1. Selective bond distances and angles are given in Table 2.

CCDC: 1828500, **1**; 1544271, **2**.

Table 1　Crystal data and structure refinement for MOF 1 and 2

MOF	1	2
Empirical formula	$C_{72}H_{86}Cd_2N_4O_{13}$	$C_{33}H_{35}CdN_2O_8S$
Formula weight	1 440.24	732.09
Crystal system	Monoclinic	Monoclinic
Space group	*P*2/*n*	*C*2/*c*
a / nm	0.929 35(4)	1.573 7(4)
b / nm	2.060 37(9)	2.065 6(5)
c / nm	1.808 72(8)	2.201 6(6)
β / (°)	99.194 0(10)	110.369(7)
V / nm^3	3.418 9(3)	6.709(3)
Z	2	8
D_c / (g·cm^{-3})	1.399	1.305
μ / mm^{-1}	0.687	0.754
F(000)	1 492	2 680
θ range /(°)	2.282~27.643	2.19~27.54
Completeness to θ=27.54° / %	99.8	97.7
Total reflection, unique	30 102, 7 934	7 564, 7 564
R_{int}	0.044 4	0.076 2
N_{ref}, N_{par}	7 934, 532	7 564, 362
R_1, wR_2 [$I>2\sigma(I)$]*	0.058 4, 0.157 0	0.048 2, 0.111 7
GOF on F^2	1.037	1.026
$(\Delta\rho)_{max}$, $(\Delta\rho)_{min}$ / (e·nm^{-3})	1 861, −698	1 193, −540

*$R_1=\sum||F_o|-|F_c||/\sum|F_o|$; $wR_2=[\sum w(F_o^2-F_c^2)^2/\sum wF_o^4]^{1/2}$

Table 2　Selected bond lengths (nm) and angles (°) for MOF 1 and 2

1					
Cd(1)-O(1)	0.223 9(4)	Cd(1)-N(2)#1	0.237 0(2)	Cd(1)-O(4)	0.232 4(3)
Cd(1)-N(1)	0.230 0(4)	Cd(1)-O(4)#3	0.238 8(4)	Cd(1)-O(3)	0.259 1(4)
Cd(1)-N(2′)	0.231 2(8)				
O(1)-Cd(1)-O(3)#2	153.27(16)	N(2)#1-Cd(1)-O(4)#3	86.8(4)	O(1)-Cd(1)-N(2)#1	85.7(5)

Continued Table 2

N(1)-Cd(1)-O(3)#2	85.13(13)	O(4)#2-Cd(1)-O(4)#3	70.17(14)	N(1)-Cd(1)-O(4)#2	90.17(13)
O(4)#2-Cd(1)-O(3)#2	51.65(13)	N(1)-Cd(1)-O(4)#3	94.66(14)	O(1)-Cd(1)-O(4)#2	154.59(16)
N(2)#1-Cd(1)-O(3)#2	92.6(4)	O(1)-Cd(1)-O(4)#3	84.78(14)	N(1)-Cd(1)-N(2′)#1	165.8(2)
O(4)#3-Cd(1)-O(3)#2	121.80(12)	O(4)#2-Cd(1)-N(2)#1	88.6(5)	O(1)-Cd(1)-N(2′)#1	90.1(2)
O(1)-Cd(1)-N(1)	96.22(14)	N(1)-Cd(1)-N(2)#1	177.7(4)		
		2			
Cd(1)-N(1)	0.220 8(3)	Cd(1)-O(2)#3	0.222 9(2)	Cd(1)-O(6)	0.232 4(3)
Cd(1)-O(1)#2	0.222 0(3)	Cd(1)-O(5)#4	0.225 0(3)	Cd(1)-Cd(1)#4	0.310 73(9)
N(1)-Cd(1)-O(1)#2	99.51(10)	O(1)#2-Cd(1)-O(5)#4	90.17(10)	O(2)#3-Cd(1)-O(6)	82.82(10)
N(1)-Cd(1)-O(2)#3	99.64(10)	O(2)#3-Cd(1)-O(5)#4	92.80(10)	O(5)#4-Cd(1)-O(6)	156.80(11)
O(1)#2-Cd(1)-O(2)#3	157.92(9)	N(1)-Cd(1)-O(6)	91.31(11)		
N(1)-Cd(1)-O(5)#4	111.89(11)	O(1)#2-Cd(1)-O(6)	85.86(10)		

Symmetry codes: #1: *x*, *y*−1, *z*; #2: *x*+1, *y*, *z*; #3: −*x*+1/2, *y*, −*z*+3/2 for **1**; #1: −*x*+3/2, −*y*+1/2, −*z*+2 ; #2: *x*−1/2, *y*−1/2, *z*; #3: −*x*+3/2, −*y*+1/2, −*z*+1; #4: −*x*+1, −*y*, −*z*+1; #5: *x*+1/2, *y*+1/2, *z* for **2**.

2 Results and discussion

2.1 Crystallographic description

2.1.1 Description of the crystal structure of {[Cd(L)(fma)]·0.5H_2O}$_n$ (**1**)

Single-crystal structure analysis reveals that **1** crystallizes in the monoclinic crystal system with *P*2/*n* space group. The asymmetric unit of **1** consists of one Cd(Ⅱ) metal center, one L ligand, one fma^{2-} anion and a half of lattice H_2O molecule. Each Cd(Ⅱ) center is seven-coordinated by five oxygen atoms from three different fma^{2-} ligands and two nitrogen atoms from two different L ligands to form a pentagonal bipyramid (Fig.1a). The five oxygen atoms from three fma^{2-}

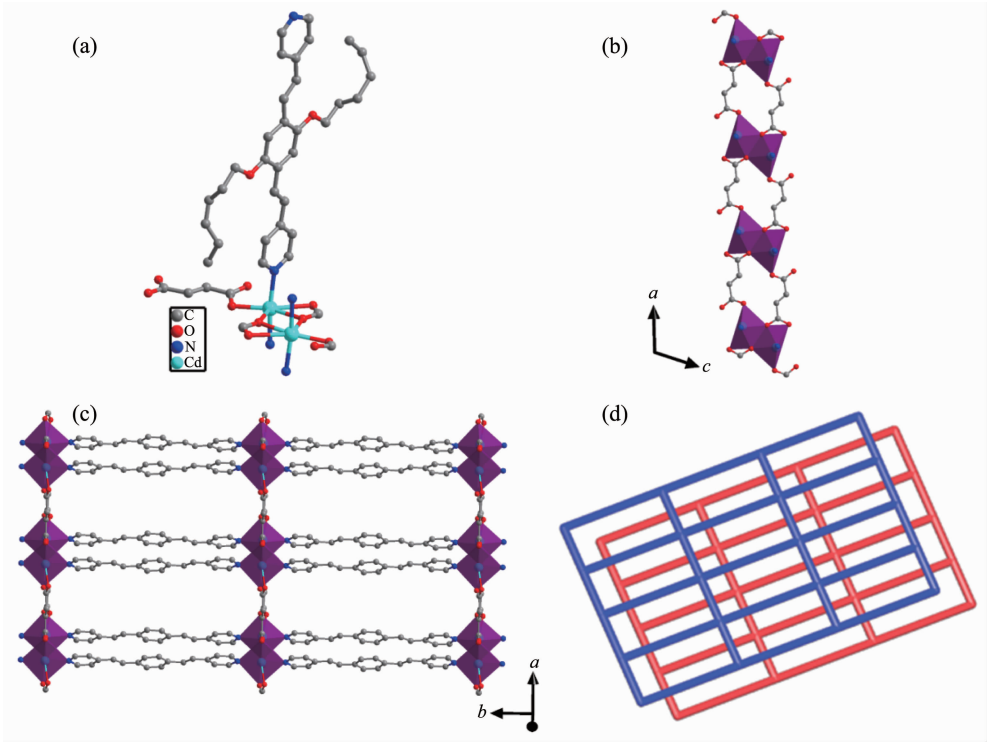

Fig.1 (a) Coordination environment of **1**; (b) 1D chain constructed by fma^{2-} ligand and cadmium ion; (c) Views of 2D sheets; (d) Schematic representation of an *sql* poly-catenation of **1**

ligands locate in the equatorial plane, and two N atoms from two L ligands occupy the axial positions. The carboxylate groups adopt two coordination modes (Mode Ⅰ and Ⅱ of Fig.2) to connect two Cd centers to generate $[Cd_2(CO_2)_4]$ as a secondary building unit (SBU). The fma^{2-} ligands connect SBUs to form 1D chains (Fig.1b). These 1D chains are connected by L ligand in the axial direction to form the 2D sheet (Fig. 1c).

To better understand the nature of this intricate framework, we apply a topological approach, which reduces multidimensional structures to simple nodes and connection nets. The SBUs can be regarded as 4-connected nodes and the two ligands act as linkers. Thus, the whole structure can be characterized as a non-interpenetrated 2D+2D → 2D parallel stacked 4-connected *sql* network with the point symbol of $\{4^4.6^2\}$ (Fig.1d).

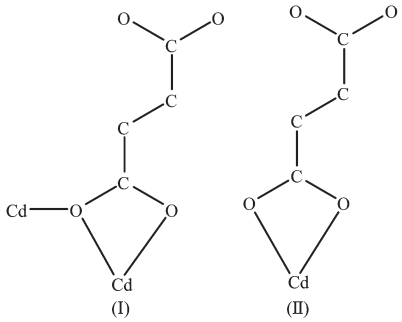

Fig.2　Coordination modes of carboxylic groups in MOF **1**

2.1.2　Description of the crystal structure of $\{[Cd(L)_{0.5}(sdb)]\cdot DMF\}_n$ (**2**)

Single-crystal structure analysis reveals that **2** crystallizes in the monoclinic crystal system with C2/c space group. The asymmetric unit of **2** consists of one Cd(Ⅱ) metal center, a half of L ligand, one sdb^{2-} anion and one lattice DMF molecule, which was removed by the SQUEEZE routine in PLATON. Each Cd(Ⅱ) center is five-coordinated by four oxygen atoms from four different sdb^{2-} ligands and one nitrogen atom from one L ligand to form a square pyramid (Fig.3a). Four carboxylate groups from four different sdb^{2-} ligands connect pairs of Cd ions to generate a dinuclear Cd(Ⅱ)

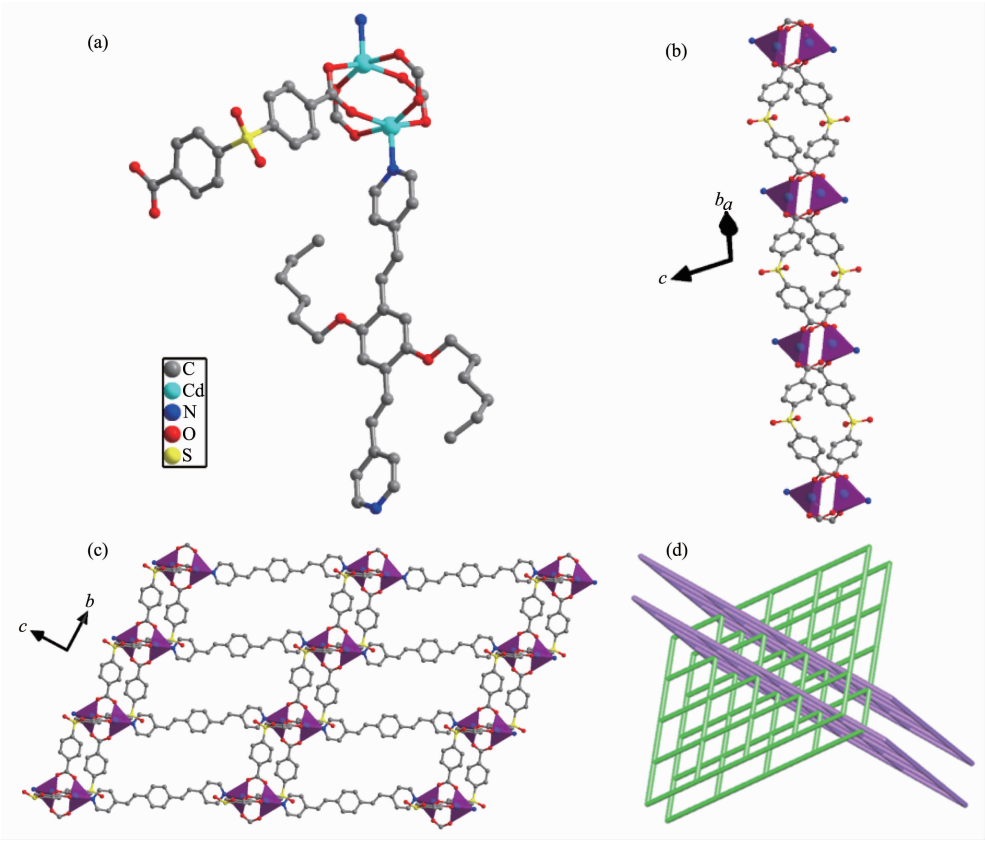

Fig.3　(a) Coordination environment of **2**; (b) 1D chain constructed by sdb^{2-} ligand and cadmium ion; (c) Views of 2D sheets; (d) Schematic representation of an *sql* poly-catenation of **2**

secondary building unit (SBU) $[Cd_2(CO_2)_4]$ in which the axial positions are occupied by L ligand. The sdb^{2-} ligands connect the $[Cd_2(CO_2)_4]$ (SBU) to form 1D chains (Fig.3b). These 1D chains are connected by L ligand in the axial direction to form the 2D sheet (Fig.3c). If the $[Cd_2(CO_2)_4]$ SBUs are regarded as 4-connected nodes and the two ligands act as linkers, the whole structure can be characterized as a interpenetrated 2D+2D → 3D inclined polycatenated 4-connected *sql* network with the point symbol of $\{4^4.6^2\}$ (Fig.3d).

2.2 Thermal stability and powder X-ray diffraction (PXRD)

To examine the thermal stabilities of **1** and **2**, TG analyses were carried out (Fig.4). The thermogravimetric curve of **1** indicating a weight loss of 1.19% (Calcd. 1.25%) was observed from 100 to 180 ℃ attributed to the loss of the one lattice water molecule. Further weight loss indicates the decomposition of coordination framework from 340 ℃. The TG thermogravimetric curve of **2** presented a 10.00% (Calcd. 9.98%) weight loss of one solvent DMF molecule from 50 to 210 ℃, and the framework started to decompose at 380 ℃. To confirm whether the crystal structures are truly representative of the bulk materials, the powder X-ray diffraction (PXRD) patterns were recorded for **1** and **2**, and they are comparable to the corresponding simulated patterns calculated from the single-crystal diffraction data (Fig.5), indicating a pure phase of each bulky sample.

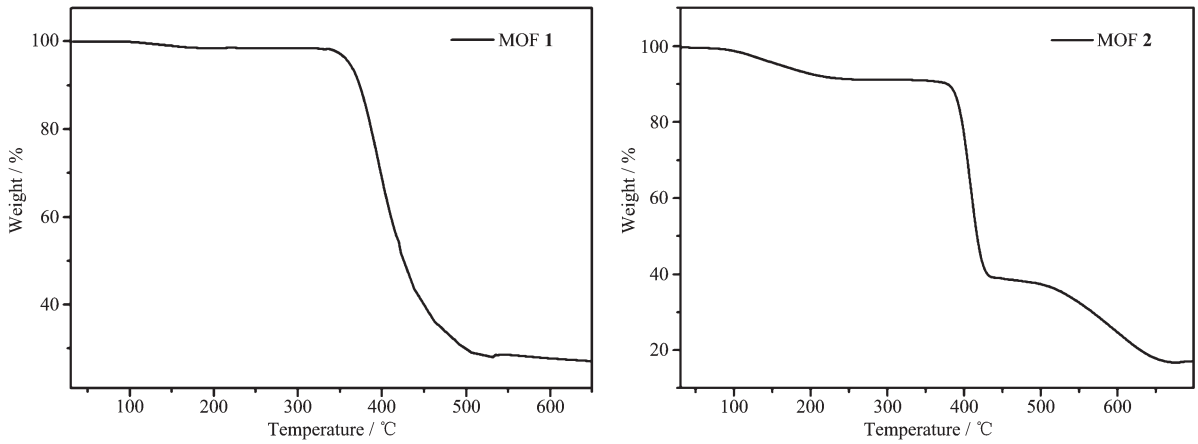

Fig.4 TG curves of MOFs **1** and **2**

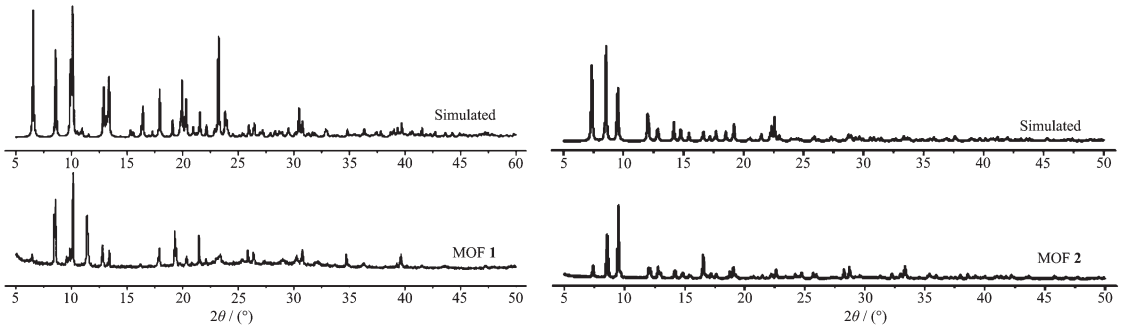

Fig.5 PXRD patterns of MOFs **1** and **2**

2.3 Metal cations and organic molecules sensing

The studies of the selectively sensing ability for different metal cations were performed. Different DMF (100 μL) solutions containing 0.05 mol·L^{-1} $G(NO_3)_x$ (G=Al^{3+}, Co^{2+}, Cr^{3+}, K^+, Mg^{2+}, Na^+, Zn^{2+}, Cu^{2+}, Fe^{3+}) were added into the suspension of MOFs **1** and **2**, respectively. To our surprise, Fe^{3+} showed an excellent quenching effect on the luminescence of MOFs **1** and **2**. There was a significant change of luminescence intensity which decreased to 99% for **1** and 96% for **2**, respectively (Fig.6). However, the luminescence quenching efficiency was not good for other cations,

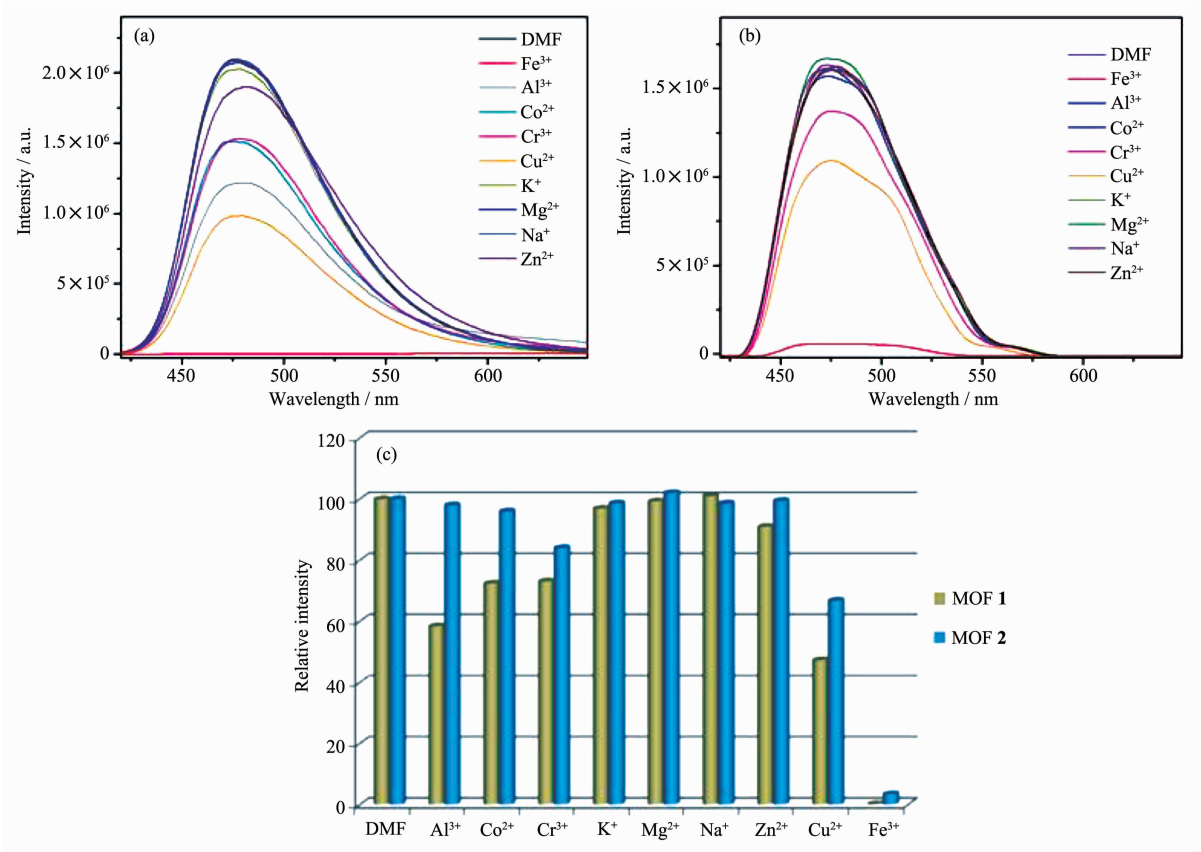

c_{metal}=0.05 mol·L^{-1}, V_{metal}=100 μL

Fig.6　Fluorescence spectra of MOFs **1** (a) and **2** (b) in DMF suspension added different metal ions; Relative emission intensity in the presence of different metal ions (c)

most for under 50%. To illuminate the possible mechanism of luminescence quenching by Fe^{3+}, we studied the liquid UV-Vis absorption spectra of Fe^{3+}, MOFs **1** and **2** (Fig.7). Obviously, Fe^{3+} ion in DMF had a wide absorption band from 270 to 450 nm, which covered the whole ranges of MOFs **1** and **2**. Therefore, the luminescence decrease of MOFs **1** and **2** after addition of Fe^{3+} can be put down to the competition of absorbing light source energy between Fe^{3+} and these two MOFs. Fe^{3+} ion filters the light adsorption of MOFs **1** and **2**. Naturally, the luminescence intensities of MOFs **1** and **2** are obviously decreased[18-21].

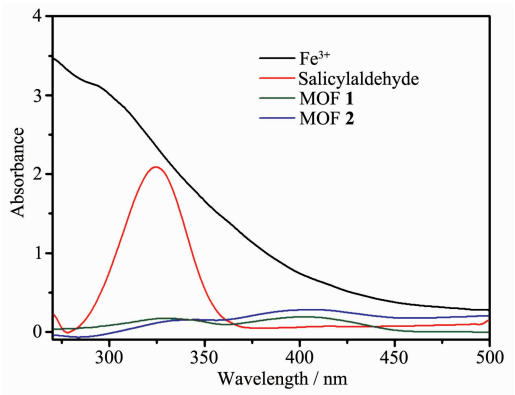

Fig.7　Liquid UV-Vis spectra of salicylaldehyde and MOFs **1** and **2**, Fe^{3+} in DMF

Furthermore, we carried out fluorescence sensing experiment to research the effect of organic molecules on MOFs **1** and **2**. A few organic molecules were chosen to investigate, such as DMF, 1,4-dioxane, *N*-methyl-2-pyrrolidone (NMP), acetonitrile, ethyl acetate (EA), isopropanol (IPA), ethanol, methanol, acetone, *tert*-butanol, salicylaldehyde. 20 μL different organic molecules mentioned above were added into the suspension of MOFs **1** and **2**, respectively. Interestingly, only salicylaldehyde shows a definite quenching effect on the luminescence of MOFs **1** and **2** (Fig.8). The quenching efficiency can reached 46% for **1** and 41% for **2**. According to the UV-Vis absorption spectrum (Fig.7), salicylaldehyde in DMF has an

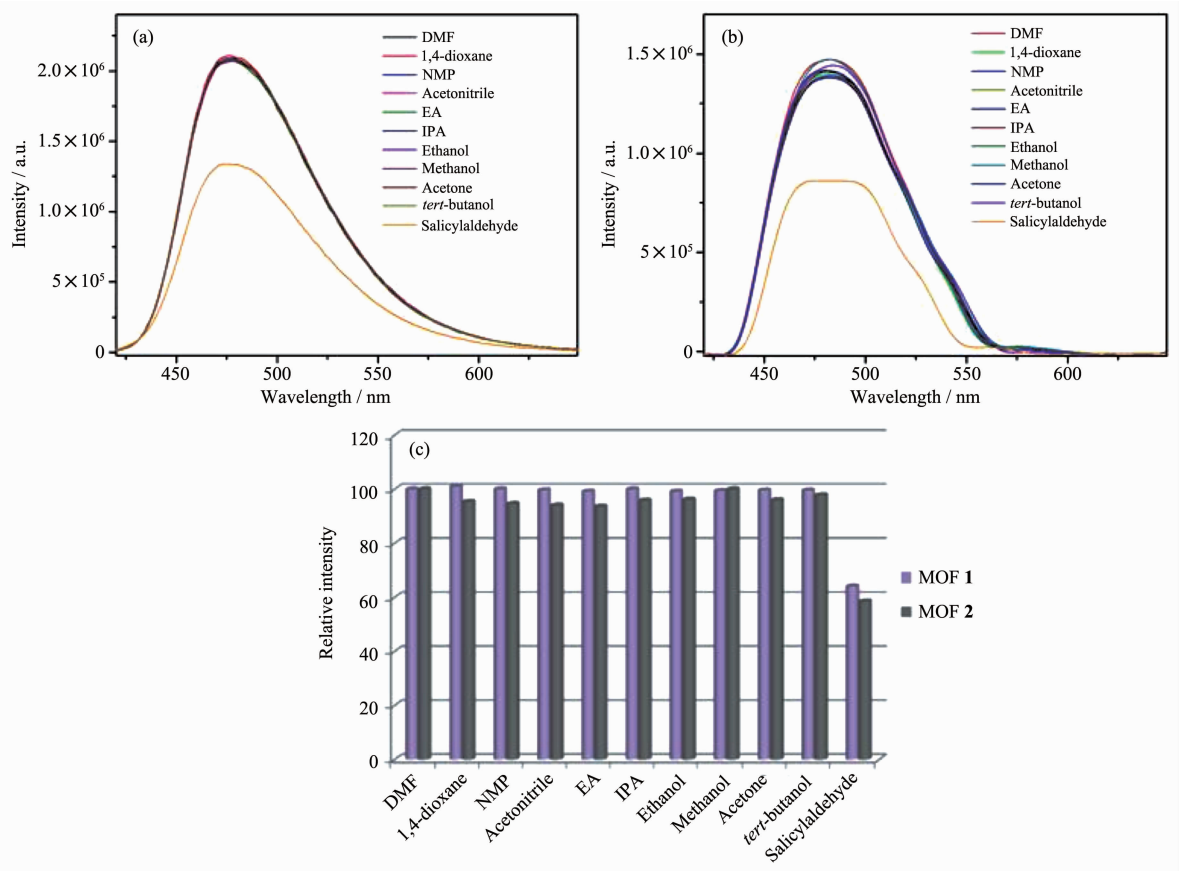

Fig.8 Fluorescence spectra of MOFs **1** (a) and **2** (b) in DMF suspension added 20 μL pure organic molecules; (c) Relative emission intensity in the presence of pure organic molecules

absorption band in 325 nm, it covers partial absorption band of MOFs **1** and **2**. Hence, the luminescent intensity of them was decreased partly.

3 Conclusions

In summary, tw o new cadmium metal-organic frameworks have been successfully synthesized. Luminescence sensing measurements indicate that they can be developed as highly selective probes for detection of Fe^{3+} in DMF solutions. We presumed that the luminescence quenching effect depended on the UV-Vis competitive adsorption. We also explored the potential of MOFs **1** and **2** for detecting organic molecules. The results show that salicylaldehyde presents the best quenching effect on these two MOFs.

References:

[1] Zhu J, Usov P M, Celis-Salazar P J, et al. *J. Am. Chem. Soc.*, **2018**,**140**:993-999

[2] Erkartal M, Sen U. *ACS Appl. Mater. Interfaces*, **2018**,**10**:787-793

[3] Jiang J, Furukawa H, Zhang Y B, et al. *J. Am. Chem. Soc.*, **2016**,**138**:10244-10251

[4] ZHANG Chun-Li(张春丽), ZHENG He-Gen(郑和根), et al. *Chinese J. Struct. Chem.*(结构化学), **2016**,**35**(7):1070-1076

[5] Liu J B, Zhuang Y X, Wang L, et al. *ACS Appl. Mater. Interfaces*, **2018**,**10**:1802-1808

[6] ZHANG Chun-Li(张春丽), QIN Ling(覃玲), ZHENG He-Gen(郑和根), et al. *Chinese J. Inorg. Chem.*(无机化学学报), **2013**,**29**(11):2347-2350

[7] Liu M J, Gao K, Fan Y R, et al. *Chem. Eur. J.*, **2018**,**24**:1416-1422

[8] Wang Y, Huang N Y, Shen J Q, et al. *J. Am. Chem. Soc.*, **2018**,**140**:38-44

[9] Xiao J D, Yu S H, Jiang H L, et al. *Angew. Chem., Int. Ed.*, **2018**,**57**:1103-1110

[10]Chen Y, Wang Z U, Wang H, et al. *J. Am. Chem. Soc.*, **2017**,**139**:2035-2041

[11]Sharma V, De D, Pal S, et al. *Inorg. Chem.*, **2017**,**56**:8847-8853

[12]Yang N N, Fang J J, Sui Q, et al. *ACS Appl. Mater. Interfaces*, **2018**,**10**:2735-2741

[13]Luo X, Zhang X, Duan Y L, et al. *Dalton Trans.*, **2017**,**46**:6303-6309

[14]Yan W, Zhang C L, Chen S G, et al. *ACS Appl. Mater. Interfaces*, **2017**,**9**:1629-1636

[15]Chen S G, Shi Z Z, Qin L, et al. *Cryst. Growth Des.*, **2017**,**17**:67-73

[16]Shen K, Qin L, Zheng H G. *Dalton Trans.*, **2016**,**45**:16205-16210

[17]Sheldrick G M. *SHELXL*-97, *Program for the Refinement of Crystal Structure*, University of Göttingen, Germany, **1997**.

[18]Sun W, Wang J, Zhang G, et al. *RSC Adv.*, **2014**,**4**:55252-55258

[19]Xu H, Liu F, Cui Y J, et al. *Chem. Commun.*, **2011**,**47**:3153-3160

[20]Wen G X, Han M L, Wu X Q, et al. *Dalton Trans.*, **2016**,**45**:15492-15498

[21]Yi F Y, Li J P, Wu D, et al. *Chem. Eur. J.*, **2015**,**21**:11475-11482